Shaping Magnetic Energy Density and Flux via Azimuthally Polarized Vortex Pairs

M.Udhayakumar[1*], M. Manikandan[1], Kumar Kumarappan[1], K.B. Rajesh[2]

[1]Department of Physics, VSB College of Engineering Technical Campus, Coimbatore, Tamil Nadu, India

[2*]Department of Physics, Chikkanna Government Arts College, Tiruppur, Tamilnadu, India

Abstract

In this article, magnetic field distribution and energy flux near the focus of an tight focused of azimuthally polarized Gaussian beam with nested pair of vortices is investigated theoretically by vector diffraction theory. Results show that the magnetization field distribution in the focal region can be altered considerably through phase modulation and by changing location of the vortices nested in the azimuthally polarized Gaussian Beam. It is also observed that for well optimized phase filter in the pupil plane, one can tune the magnetization field distribution from a twin splitted central null shaped into flattop profile and then to sharper focus upon suitably positioning the vortex pair nested in the Gaussian beam. The calculated energy flow pattern reveals that the total poynting vector is dominated by the transverse component when the distance between the vortex pair are small whereas it is dominated by longitudinal component when it is increased.

Keywords

Pair of Vortices, Focusing properties, Vector diffraction theory, Inverse Faraday Effect, High NA lens.

1. Introduction

Recently, the manipulation of the electric field and polarization near the focus of high–numerical-aperture (NA) optical systems has attracted significant attention due to its wide range of applications, including optical trapping and particle manipulation [1–2], high-resolution microscopy [3], optical data storage [4], and electron acceleration [5]. Numerous approaches have been proposed to engineer focal fields, such as the introduction of amplitude and phase modulations, enabling the generation of sharper focal spots [6–7], multiple focal spots [8–11], flat-top focal distributions [12], optical chains [13–14], optical channels [15–16], and optical cages [17]. However, several emerging applications—such as magnetic resonance microscopy [20], magneto-optical data storage [21], atom trapping [22], and all-optical magnetic recording [23]—critically rely on the magnetic field distribution in the focal region of high-NA focusing systems. In this work, we propose a method to tailor the magnetic field distribution near the focus of a tightly focused azimuthally polarized Gaussian beam embedded with a pair of optical vortices. By employing appropriate phase modulation and precisely tuning the separation between the vortex pair, controllable magnetization field distributions in the focal region are achieved.

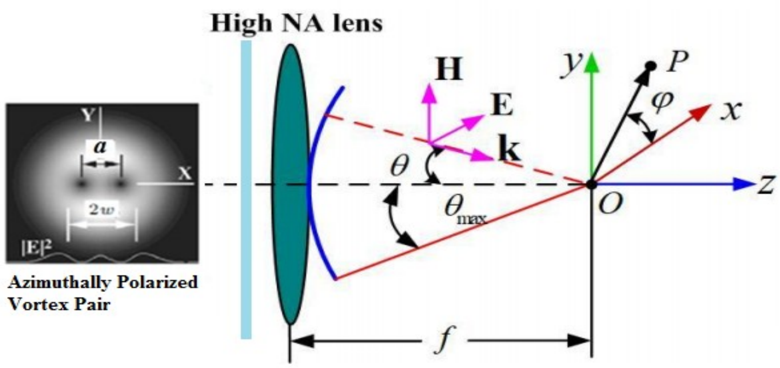

Figure 1.Illustration of a high-numerical-aperture system.

2. Theory

The polarization state of light can be represented mathematically as a linear combination of two mutually orthogonal basis vectors. In the case of a generalized cylindrical vector (CV) beam, the state of polarization is formulated as a superposition of these orthogonal components. [24].

$$E_0 = \frac{A_0}{\sqrt{2}}\left\{\exp[i(\varphi+\varphi_0)]e_r + \exp[-i(\varphi+\varphi_0)]e_l\right\} = A_0\left[\cos(\varphi+\varphi_0)e_x + \cos(\varphi+\varphi_0)e_y\right] \rightarrow (1)$$

Here, $A0$ is a constant amplitude factor, ϕ denotes the azimuthal angle, and ϕ0 represents the initial phase. The vectors er and el correspond to the unit vectors of right-handed and left-handed circular polarization, respectively, whereas ex and ey denote the unit vectors associated with linear polarization along the x- and y-axes. For the incident optical field defined in Eq. (1), the resulting three-dimensional electric and magnetic field distributions in the focal region can be obtained within the cylindrical coordinate framework (r, φ, z) as [25]

$$\begin{bmatrix} E(r,\phi,z) \\ H(r,\phi,z) \end{bmatrix} = \frac{-ikf}{2\pi}\int_0^{\alpha}\int_0^{2\pi} \sqrt{\cos\theta}\, l(\theta)\sin\theta \begin{bmatrix} M_E \\ M_H \end{bmatrix} \exp(ik_0 \cdot r)\, d\theta\, d\varphi \rightarrow (2)$$

In this formulation, the wave number is defined as k=2π/λ where λ denotes the free-space wavelength. The parameter f represents the focal length of the objective lens. The maximum convergence angle is given by α= arcsin(NA/n) with the numerical aperture NA=0.9 and the refractive index in the image space n=1. The angles θ and φ correspond to the polar (with respect to the z axis) and azimuthal (with respect to the x-axis) directions, respectively. The vectors M_E and M_H denote the electric and magnetic polarization components of the propagating field in the image space. The unit wave-vector direction is expressed as; k_0 = (-sinθ cosφ, -sinθsinφ, cosθ) An arbitrary point in the image space is described by the position vector r = (rcosφ, rsinφ, z) while , *l(θ)* represents the relative amplitude distribution of the incident optical field at the entrance pupil. For a pair of optical vortices with topological charge *m*=1, symmetrically positioned located at *x*=±*a*, within the transverse plane of a Gaussian host beam, the resulting electric field in cylindrical coordinates (*r, φ, 0*) can be written as [26].

$$l(\theta) = \exp\left(-\frac{r^2}{\omega}\right)\left[r\exp\left(i\varphi\right) - d\right]\left[r\exp\left(i\varphi\right) + d\right] \rightarrow (3)$$

Where ω =w0/r0 is called relative waist *r* and ϕ correspond to the radial coordinate and azimuthal angle in a polar coordinate system, respectively. The parameter *w0* is a constant that defines the beam waist. The separation between the two vortices is controlled by the parameter aaa. When a=0, the vortices coincide, and the resulting beam reduces to a single vortex beam with a topological charge m=2. The Electric and magnetic polarization vectors in terms of M_E *and* M_H can be respectively derived as

$$M_E = \begin{bmatrix} M_E^x \\ M_E^y \\ M_E^z \end{bmatrix} = \begin{bmatrix} -\sin\varphi_0\sin\varphi + \cos\varphi_0\cos\theta\cos\varphi \\ \sin\varphi_0\cos\varphi + \cos\varphi_0\cos\theta\sin\varphi \\ \cos\varphi_0\sin\theta \end{bmatrix} \quad M_H = \sqrt{\frac{\varepsilon}{\mu}}\begin{bmatrix} M_H^x \\ M_H^y \\ M_H^z \end{bmatrix} = \begin{bmatrix} -\cos\varphi_0\sin\varphi - \sin\varphi_0\cos\theta\cos\varphi \\ \cos\varphi_0\cos\varphi - \sin\varphi_0\cos\theta\sin\varphi \\ -\sin\varphi_0\sin\theta \end{bmatrix}$$

where, ε and μ the dielectric permittivity and magnetic permeability of the image space be denoted by the relevant material parameters. Using the three-dimensional electric and magnetic field vectors, the energy flow is characterized by the time-averaged Poynting vector. [25]:

$$P\alpha\frac{c}{8\pi}\mathrm{Re}(\mathrm{E}\times\mathrm{H}^*)$$

in this context, the asterisk indicates complex conjugation. Using this definition, the magnetic field distribution and the associated energy flow in the focal region of tightly focused circularly polarized beams can be determined.

3. Results and discussion

Without loss of generality and validity, it is proposed that the parameters are chosen as λ = 632.8 nm, w =2 mm, f =2 mm, NA= 0.9, m = 1.In order to achieve splitting of magnetization focal segment a three belt binary phase optical element is introduced into the optical focusing system. The transmission function *T(*θ*)* of the specially designed three-belt filter is written as

$$\mathrm{T}(\theta)=\begin{cases}1, for 0<\theta<\theta_1, \theta_2<\theta<\theta_{\max}, \\ -1 for \theta_1<\theta<\theta_2\end{cases}$$

the angles θ_1 and θ_2, corresponding to two radial positions r_1 and r_2(ri =sinθi/NA, i =1, 2), respectively. Our aim is to search an optimum set of parameters $\{r_i, \theta_i\}$ to satisfy the above goals by virtue of a series of iterative process. We here give an optimized example that is characterized by the following two angles θ_1=5.43° and θ_2=35.36° and the corresponding radial positions are given by r_1=0.0996 and r_2=0.6092, respectively. The effect of location of the vortices on the beam pattern in the focal region is shown in fig (2). It is observed that when a=0, the vortex overlaps each other and generates beam with topological charge *m= 2.* The corresponding magnetization intensity generated is found to be a splitted magnetization hole with null intensity at the centre separated by distance of 1.5λ, having a FWHM of 0.76λ and depth of focus around 1.1λ for each is observed. However setting a=0.31, an axially splitted magnetization flattop profile separated by a distance of 1.2λ with FWHM of 0.852λ and focal depth of 1.3λ are observed. Further increasing a to 0.8 makes magnetization spots sharper with radial FWHM as 0.32λ and its corresponding depth of focus as 1.1λ is obtained. Thus it is noted that Increase location of the vortices continuously, the magnetization pattern changes considerably.

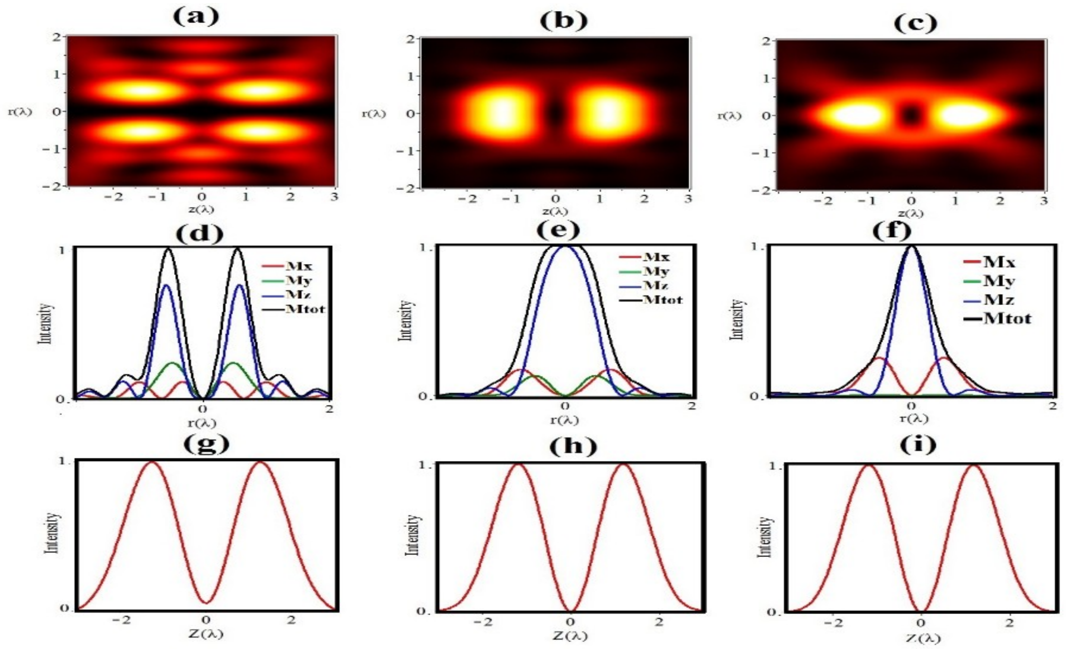

Fig. 2 Magnetization distributions in the focal plane as a Gaussian beam with a pair of vortices of same charges focused by a high NA objective. (a) a = 0; (b) a = 0.31w; (c) a = 0.8w. The other parameters are chosen as λ = 632.8 nm, w =2 mm, f =2 mm, NA= 0.95.

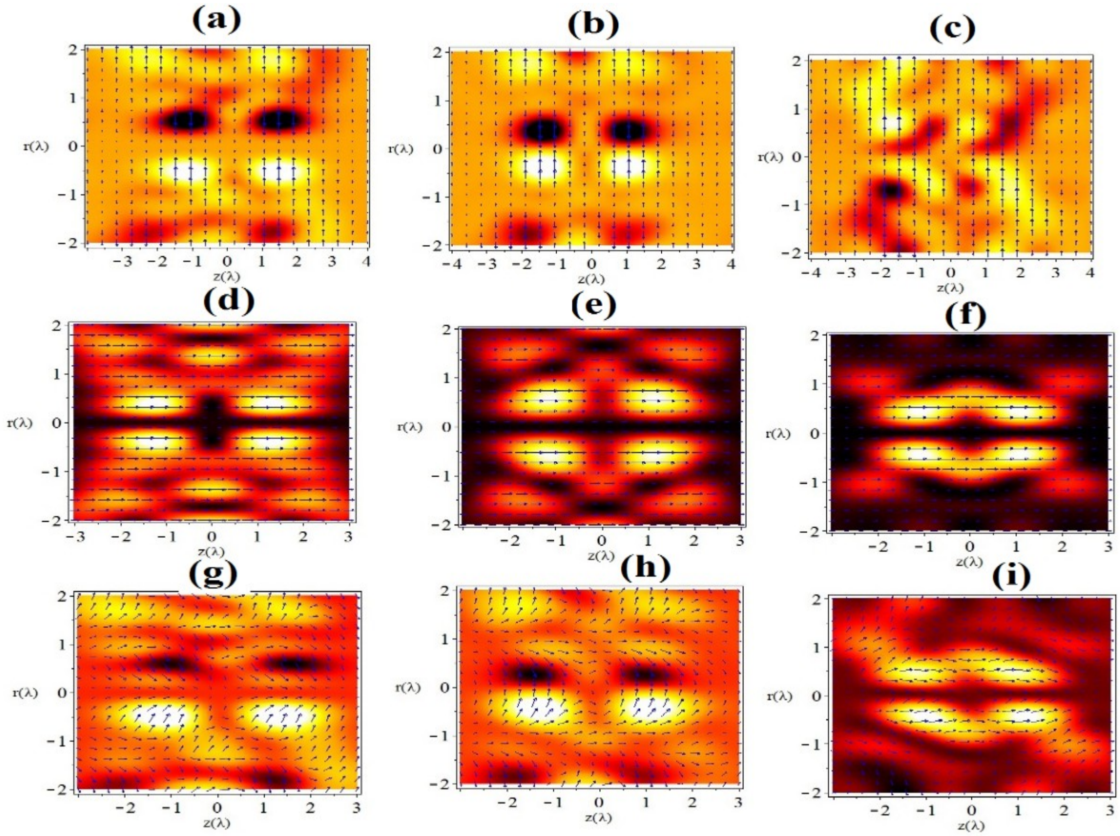

Figure 3 shows the normalized Poynting vectors in the through-focus plane

The study of energy flow in the focal region of an aplanatic optical system has always attracted research interest [27-28] due to the potential applications like manipulating and transporting absorptive particles. Figure (3) shows the energy flow pattern along the focus for the after mentioned cases. The upper and middle rows respectively shows the transverse and longitudinal components of the normalized Poynting vectors whereas the last row shows the total energy flow. We noted that for all the cases considered 1.e *a*=0, 0.31 and 0.8, the transverse and longitudinal components of the normalized Poynting vectors exhibits dual hollow shaped pattern. We noted that transverse energy flow is reversed before and after the focus and its found to be inwardly and outwardly along the radial direction, the condition which in general transports absorptive particles in the optical axis or away from it. It is also noted that when the=0 and 0.31 the total pointing vector is dominated by the transverse component whereas it is dominated by longitudinal component when a=0.8.

4. Conclusion

In conclusion, a new method to manipulate magnetization focal pattern utilizing tightly focused phase modulated azimuthally polarized Gaussian beam nested with a pair of vortex is demonstrated numerically on the basis of Vector Diffraction Theory. Results show that the magnetization field distribution in the focal region can be altered considerably through phase modulation and by changing location of the vortices nested in the azimuthally polarized Gaussian Beam. It is also noted that the total poynting vector is dominated by the transverse component when the distance between the vortex pair are small whereas it is dominated by longitudinal component when it is increased.

References

[1] Y. Zhang, J. Wang, J. Shen, Z. Man, W. Shi, C. Min, G. Yuan, S. Zhu, H.P. Urbach, X. Yuan, , Plasmonic Hybridization Induced Trapping and Manipulation of a Single Au Nanowire on a Metallic Surface *Nano Lett*. **14** , 6430-6436 (2014).

[2] C. Min, Z. Shen, J. Shen, Y. Zhang, H. Fang, G. Yuan, L. Du, S. Zhu, T. Lei, X. Yuan, Focused plasmonic trapping of metallic particles, *Nat. Commun.* **4** ,2891(2013).

[3] Y. Kozawa, D. Matsunaga, and S. Sato, "Superresolution imaging via polarization-dependent excitation of tightly focused light," Optica 5, 86–92 (2018).

[4] Y. Zhang and J. Bai, "Focusing properties of radially polarized annular Gaussian beams," Opt. Express 17, 3698–3706 (2009).

[5] J. Xu, Z. J. Yang, J. X. Li, and W. P. Zang, "Engineering focal field distribution of tightly focused beams by phase modulation," Laser Phys. Lett. 14, 025301 (2017).

[6] G. Y. Chen, F. Song, and H. T. Wang, "Strong longitudinally polarized fields from tightly focused radially polarized beams," Opt. Lett. 38, 3937–3940 (2013).

[7] Z. Man, Z. Bai, S. Zhang, J. Li, X. Li, X. Ge, Y. Zhang, and S. Fu, "Tailoring focal field distributions by vectorial beam modulation," J. Opt. Soc. Am. A 35, 1014–1020 (2018).

[8] M. Cai, C. Tu, H. Zhang, S. Qian, K. Lou, Y. Li, and H. T. Wang, "Engineering the optical magnetic field of a tightly focused vector beam," Opt. Express 21, 31469–31482 (2013).

[9] P. Li, X. Guo, S. Qi, L. Han, Y. Zhang, S. Liu, Y. Li, and J. Zhao, "Optical magnetic field enhancement via tightly focused structured light," Sci. Rep. 8, 9831 (2018).

[10] H. Wang, L. Shi, B. Lukyanchuk, C. Sheppard, and C. T. Chong, "Creation of a needle of longitudinally polarized light in vacuum using binary optics," Nat. Photonics 2, 501–505 (2008).

[11] Z. Man, C. Min, L. Du, Y. Zhang, S. Zhu, and X. Yuan, "Manipulating the focal field distribution by complex vector beam modulation," Opt. Express 26, 874–882 (2016).

ISSN : 1671-6841

[12] X. Wang, B. Zhu, Y. Dong, S. Wang, Z. Zhu, F. Bo, and X. Li, “Tailoring optical focal fields with spatially varying polarization,” Opt. Express 25, 26844–26852 (2017).

[13] Y. Zhao, Q. Zhan, Y. Zhang, and Y. P. Li, “Generation of a longitudinally polarized field with a circularly polarized beam,” Opt. Lett. 30, 848–850 (2005).

[14] J. Wang, W. Chen, and Q. Zhan, “Manipulation of longitudinal fields in high-numerical-aperture focusing,” J. Opt. 14, 055004 (2012).

[15] J. Guan, N. Liu, C. Chen, X. Huang, J. Tan, J. Lin, and P. Jin, “Magneto-optical response enhancement using structured optical fields,” Opt. Express 26, 24075–24088 (2018).

[16] L. Wei and H. P. Urbach, “Focal field shaping of high-numerical-aperture systems,” J. Opt. 18, 065608 (2016).

[17] Z. Man, Z. Bai, J. Li, S. Zhang, X. Li, Y. Zhang, X. Ge, and S. Fu, “Tailoring three-dimensional focal field distributions using vector beams,” Appl. Opt. 57, 3592–3597 (2018).

[18] N. Bokor and N. Davidson, “Tight focusing of radially polarized light,” Opt. Lett. 29, 1968–1970 (2004).

[19] S. Yan, B. Yao, and R. Rupp, “Focusing properties of radially polarized beams,” Opt. Express 19, 673–678 (2011).

[20] M. S. Grinolds et al., “Nanoscale magnetic imaging of a single electron spin under ambient conditions,” Nat. Nanotechnol. 9, 279–284 (2014).

[21] P. Zijlstra, J. W. M. Chon, and M. Gu, “Five-dimensional optical recording mediated by surface plasmons in gold nanorods,” Nature 459, 410–413 (2009).

[22] P. Schneeweiss, F. Le Kien, and A. Rauschenbeutel, “Nanofiber-based atom trapping and manipulation,” New J. Phys. 16, 013014 (2014).

[23] A. R. Khorsand et al., “Role of magnetic dipoles in the optical response of split-ring resonators,” Phys. Rev. Lett. 108, 127205 (2012).

[24] Q. Zhan, “Cylindrical vector beams: from mathematical concepts to applications,” Adv. Opt. Photon. 1, 1–57 (2009).

[25] B. Richards and E. Wolf, “Electromagnetic diffraction in optical systems. II. Structure of the image field in an aplanatic system,” Proc. R. Soc. London Ser. A 253, 358–379 (1959).

[26] Z. Chen, J. Pu, and D. Zhao, “Focusing properties of vector beams in high numerical aperture systems,” Phys. Lett. A 375, 2958–2963 (2011).

[27] X. Jiao, S. Liu, Q. Wang, X. Gan, P. Li, and J. Zhao, “Enhancement of longitudinal fields by tightly focused vector beams,” Opt. Lett. 37, 1041–1043 (2012).

[28] X.-Z. Gao, Y. Pan, G.-L. Zhang, M.-D. Zhao, Z.-C. Ren, C.-G. Tu, Y.-N. Li, and H.-T. Wang, "Redistributing the energy flow of tightly focused ellipticity-variant vector optical fields," Photon. Res. 5, 640–648 (2017).